0Metallophysics and Advanced Technologies
Металофіз. новітні технол.
Metallofiz. Noveishie Tekhnol.
2026, vol. 48, No. 3, pp. 307–319
https://doi.org/10.15407/mfint.48.03.0307
Reprints available directly from the publisher

PACS numbers: 07.35.+k, 74.45.+c, 74.50.+r, 74.62.Fj, 74.70.Ad, 74.78.-w, 74.81.Bd

Superconducting Properties of Ta and MoRe under Torsional Strain and High Pressure

V. Tarenkov[*,**], D. Mindich[***], V. Dmytrenko[*], O. Zhitlukhina[*,****], V. Krivoruchko[*], O. Kalenyuk[**,***], D. Shapovalov[**], V. Shamaev[*****], and A. Shapovalov[**,***]

[*]*Donetsk Institute for Physics and Engineering Named after O. O. Galkin, N.A.S. of Ukraine, 46 Nauky Ave., UA-03028 Kyiv, Ukraine*
[**]*G. V. Kurdyumov Institute for Metal Physics, N.A.S. of Ukraine, 36 Academician Vernadsky Blvd., UA-03142 Kyiv, Ukraine*
[***]*Kyiv Academic University, N.A.S. and M.E.S. of Ukraine, 36 Academician Vernadsky Blvd., UA-03142 Kyiv, Ukraine*
[****]*Centre for Nanotechnology and Advanced Materials, Faculty of Mathematics, Physics and Informatics, Comenius University Bratislava, Mlynská Dolina, 84248 Bratislava, Slovak Republic*
[*****]*Donetsk National Technical University, 76 Sambirska Str., UA-82111 Drohobych, Ukraine*

The twistronics paradigm, within which the rotation of crystal layers is used to engineer electronic properties, has revolutionized the study of two-dimensional quantum materials. However, the extension of this concept to

Corresponding author: Andriy Petrovych Shapovalov
E-mail: shapovalovap@gmail.com

Citation: V. Tarenkov, D. Mindich, V. Dmytrenko, O. Zhitlukhina, V. Krivoruchko, O. Kalenyuk, D. Shapovalov, V. Shamaev, and A. Shapovalov, Superconducting Properties of Ta and MoRe under Torsional Strain and High Pressure, *Metallofiz. Noveishie Tekhnol.*, **48**, No. 3: 307–319 (2026). DOI: 10.15407/mfint.48.03.0307

three-dimensional bulk systems, where structural manipulation is inherently more complex, still requires further investigation. In this paper, we analyse the possibility of applying twistronics principles to bulk superconducting metals, namely, Ta (a classical type-I superconductor) and MoRe (a type-II superconductor), by means of the combined extreme torsional stress and hydrostatic pressure. Our results show that the superconducting properties of both materials, as determined by the ratio of the superconducting gap to the critical temperature, increase systematically under this dual loading. We believe that macroscopic torsion is a promising way to extend twistronics concepts to bulk superconductors and to engineering mechanically their superconducting properties.

Key words: twistronics, hydrostatic pressure, torsional stress, superconducting characteristics, amorphization.

Парадигма твістроніки, в якій використовується обертання кристалічних шарів для інженерії електронних властивостей, зробила революцію у вивченні двовимірних квантових матеріялів. Однак поширення цієї концепції на тривимірні об'ємні системи, де структурна маніпуляція є за своєю суттю складнішою, ще потребує свого дослідження. В даній роботі ми аналізуємо можливість застосування принципів твістроніки до об'ємних надпровідних металів, — Ta (класичний надпровідник першого типу) та MoRe (надпровідник другого типу), — за допомогою комбінованого екстремального крутильного напруження та гідростатичного тиску. Наші результати показують, що надпровідні властивості обох матеріялів, що визначаються відношенням ширини надпровідної щілини до критичної температури, систематично зростають за цього подвійного навантаження. Ми вважаємо, що макроскопічне кручення є перспективним шляхом поширення концепцій твістроніки на об'ємні надпровідники та механічної інженерії їхніх надпровідних властивостей.

Ключові слова: твістроніка, гідростатичний тиск, крутильне напруження, надпровідні характеристики, аморфізація.

(Received 12 March, 2026; in final version, 13 March, 2026)

1. INTRODUCTION

The exploration of quantum materials through controlled structural manipulation has emerged as a dominant paradigm in condensed matter physics. Among the most exciting developments in this field is twistronics, the deliberate rotation of crystalline layers to create long-period moiré superlattices. This approach gained prominence following the discovery of correlated insulating states and unconventional superconductivity in magic-angle twisted bilayer graphene [1, 2]. The core principle that a simple geometric parameter (the twist angle) can dramatically reshape the electronic band structure, flatten bands, and enhance electron correlations has since been extended to a wide range of two-dimensional

(2*D*) van der Waals heterostructures, including transition metal dichalcogenides and other layered systems [3, 4]. These studies have predominantly focused on atomically thin, layered crystals where interlayer coupling can be precisely tuned *via* rotational alignment.

While the toolkit for twistronics in 2*D* materials is now rich and sophisticated, a fundamental question remains: can the twistronics paradigm, the use of rotational degrees of freedom to engineer electronic phases, be translated to bulk, three-dimensional (3*D*) quantum materials? Most conventional superconductors and strongly correlated materials are not inherently layered in a manner amenable to mechanical stacking and rotation. Yet, the potential to modulate their electronic properties *via* a 'twist' could open a vast new landscape for materials design, especially if such a twist can be induced via macroscopic mechanical deformation rather than precise nanoscale assembly.

In this work, we confront this question by applying a twistronics methodology to bulk superconducting metals. We investigate two archetypal superconductors: tantalum (a classic, elemental type-I superconductor) and molybdenum–rhenium binary alloy (a high-performance, type-II superconductor with relatively high critical temperatures and critical fields [5]). Instead of constructing van der Waals stacks, we subject disc-shaped samples of these materials to a combined extreme torsional strain and hydrostatic pressure using a large-volume press equipped with a torsional mechanism [6, 7]. This experimental configuration imposes a macroscopic twist gradient across the thickness of the disc, analogous to a continuous distribution of twist angles while simultaneously compressing the material to high pressures. The high-pressure environment also allows us to probe the interplay between mechanical deformation and electronic phase stability under conditions that significantly modify lattice parameters and electron–phonon coupling.

Our results demonstrate that the superconducting properties of both Ta and MoRe parametrized by the ratio of the energy gap Δ and the critical temperature T_c evolve systematically and non-monotonically under this combined torsional-pressure loading. We observe distinct responses between the two materials, which is attributing to their differing electronic structures, intrinsic deformation mechanisms, and phonon spectra. In general, our work suggests that mechanical structuring, particularly through controlled torsion under pressure, is a versatile, largely unexplored route to designing and discovering novel quantum states in a wide array of bulk materials.

2. HIGH-PRESSURE TORSION METHOD FOR STRUCTURAL AMORPHIZATION

The continuous pursuit of advanced materials that combine high strength, low density, excellent corrosion resistance, and sufficient

ductility drives innovation in materials processing. Among the various strategies, strain engineering has proven to be an exceptionally effective approach for manipulating fundamental mechanical properties. This is prominently realized through severe plastic deformation (SPD) techniques, which refine microstructures leading to significant property modifications [7]. A particularly notable SPD method is high-pressure torsion (HPT) [8]. In this process, the sample, typically as a disc, is subjected to intense torsional shear strain under simultaneous application of high hydrostatic pressure between two anvils. As highlighted in the literature [7, 8], HPT stands out as an ideal platform for fundamental research due to the relative ease and precision with which key parameters as imposed strain, strain rate, pressure, and temperature can be controlled. The application of gigapascal-level pressures enables the processing of a remarkably broad spectrum of materials, including those that are inherently hard or brittle, which are often challenging to deform by other means. The HPT process is exceptionally efficient at producing bulk samples with ultrafine-grained (UFG) or even nanocrystalline scale microstructures. These materials have attracted considerable interest due to their exceptional mechanical properties, which often include significantly enhanced strength compared to their coarse-grained counterparts. Furthermore, they can exhibit novel behaviours such as low-temperature superplasticity or improved creep resistance. Beyond bulk properties, careful control of HPT parameters allows for the engineering of surface characteristics, including roughness and sub-surface microstructure [7]. The functional properties of HPT-processed materials are also of great interest, opening potential applications in diverse fields such as corrosion protection, catalysis, biotechnology, thermoelectric energy conversion, and hydrogen storage.

A fascinating and less-explored consequence of the extreme shear deformation and nanostructuring induced by HPT is its profound impact on the superconducting properties of metals. The reduction of crystallinity and introduction of severe lattice disorder can markedly alter superconducting characteristics [9–13]. For instance, studies have demonstrated an increase in the superconducting critical temperature in elemental metals like rhenium and niobium [9, 10] and a MoRe alloy [13] after HPT processing. The resulting bulk nanostructured samples are polycrystalline metals with UFG microstructures, where the enhancement of T_c has been tentatively attributed to quantum size effects or to a postulated increase in the electron–phonon coupling strength.

A central hypothesis guiding this research is that the key to understanding the evolution of superconductivity under HPT lies in the amorphization of the material [14]. Conventional methods for producing amorphous metallic states, primarily in thin-film forms suitable for microelectronic devices, include techniques like vapour deposition onto

cooled substrates, particle irradiation, and ion-beam mixing [15]. The HPT method offers a distinct advantage since it can induce a crystal-to-amorphous transition directly in bulk form, circumventing limitations imposed by critical cooling rates [7, 8]. In such a state of strong disorder, two primary, non-exclusive mechanisms can influence superconductivity. The first one is a reduction in the effectiveness of electronic screening, which can weaken the phonon-mediated attractive pairing interaction due to enhanced electron–electron Coulomb repulsion, potentially suppressing T_c although sometimes enhancing it [16]. The second possibility is an increase in the effective electron–phonon coupling strength linked to the emergence of a 'boson peak' in the vibrational density of states typical for disordered systems [17, 18]. Below we compare the effect of amorphization on superconductivity produced in pure tantalum and molybdenum–rhenium alloy by HPT treatment, partly using our preliminary results for the latter material [13].

3. EXPERIMENT

Tantalum and molybdenum–rhenium alloy represent two distinct classes of superconducting materials: Ta is an elemental superconductor, while MoRe is a transition metal alloy. Their differences in crystal structure and electron–phonon coupling lead to significant variations in their superconducting parameters, making them suitable for different applications in cryogenic engineering and physics research. Tantalum has a critical temperature of about 5 K that places it among the higher-T_c elemental superconductors, though it is still firmly in the low-temperature regime requiring liquid helium cooling. In contrast, the MoRe alloy typically exhibits a higher critical temperature that depending on the specific composition (usually around 41% Re by weight) ranges between 10 K and 12 K. The higher transition temperature allows MoRe to operate at slightly higher thermal margins compared to Ta. Tantalum is a ductile metal with a high melting point. It is relatively easy to fabricate into thin films or wires, which is why it is often used in superconducting resonators and quantum computing circuits where low loss and purity are paramount. MoRe alloy is notable among high-field superconducting alloys for its ductility. In contrast to many type-II superconductors, MoRe is ductile even after heat treatment. This allows it to be drawn into wires or machined into complex shapes more easily than brittle ceramic superconductors, facilitating its use in specialized cryogenic electronics and structural superconducting components.

Thin-film layers of Ta and a MoRe alloy were deposited *via* magnetron sputtering from a target onto sitall and sapphire substrates. X-ray photoelectron spectroscopy (accurate to 5–6 at.%) verified that the film composition faithfully matched the target. For the HPT

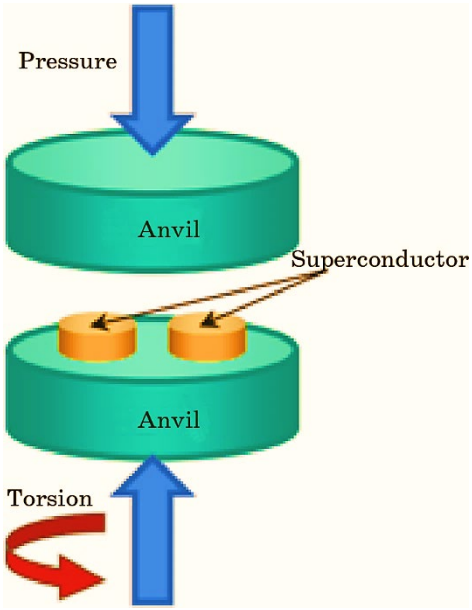

Fig. 1. Schematic diagram of HPT treating process.

treatment, 1 mm thick plates (1.5×2 mm in area) were positioned between two highly polished, high-carbon steel anvils with a diameter of 45 mm, enclosed in an outer casing. A substantial uniaxial pressure was applied. Sustaining this pressure, the upper anvil was rotated through five complete revolutions. This torsional movement caused extreme shear deformation exclusively on the upper surface of the sample. Due to friction against the anvil, the upper surface was structurally altered into a mirror-smooth finish, while the bottom surface remaining stationary against the lower anvil retained its original structural and topographical state. The test superconductor was offset from the device central axis to increase the torsional effect, and a second identical sample was added for symmetry (see Fig. 1).

4. POINT-CONTACT SPECTROSCOPY BEFORE AND AFTER HPT PROCESSING

The main objective of the work was to gain a deeper knowledge of the underlying physical mechanisms responsible for the T_c enhancement and to assess the potential of HPT as a novel, effective tool for engineering superconducting states. Previous investigations relied predominantly on macroscopic measurements, which, while valuable, provide an averaged picture. To gain a more fundamental understand-

ing, our study presents the local probe investigation of superconducting properties in samples before and after HPT processing, utilizing the powerful technique of point-contact spectroscopy. Point-contact spectroscopy was selected as the optimal diagnostic methodology, as it provides highly localized, direct analytical data regarding the amplitude and symmetry of the superconducting order parameter [19]. The analysis was conducted by establishing a micro-junction between a normal-metal (N = Ag) tip and the superconducting sample (S = Ta or MoRe). Utilizing a standard three-probe methodology, the current-voltage characteristics $I(V)$ and the differential conductance of the N/S contact $G(V) = dI(V)/dV$, the derivative of the current I through the contact with respect to the voltage bias V, were systematically measured. To preserve the pure effects of the HPT process, the natural roughness of the remaining surfaces was intentionally left untreated.

The spectroscopic data revealed a striking difference depending on the surface measured. For the surface that was in contact with the stationary lower anvil during HPT (and thus experienced minimal shear), the superconducting characteristics showed no fundamental change. In contrast, the measurements performed on the upper, mirror-smooth surface, which underwent severe shear deformation, exhibited fundamentally altered $I(V)$ and $G(V)$ curves. This direct comparison for Ta and MoRe samples presented in Figs. 2 and 3 provides convincing local

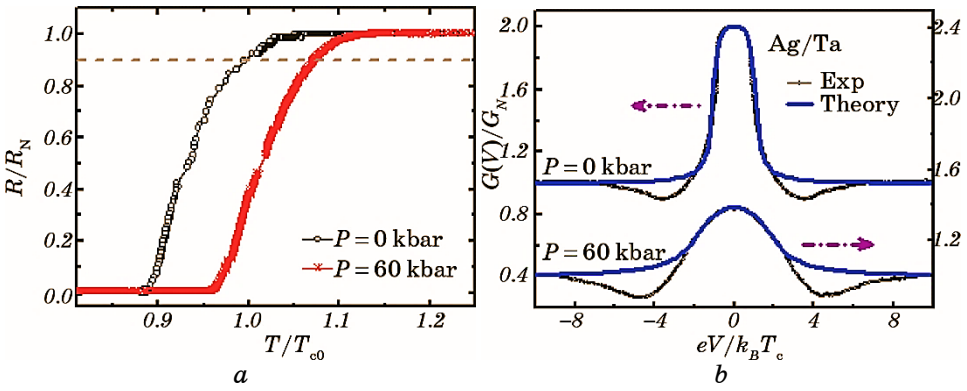

Fig. 2. Ag/Ta point contact: temperature-dependent resistances normalized to their normal-state values as functions of T/T_{c0} ratio, where $T_{c0} = T_c(P = 0$ kbar) (*a*) and differential conductance $G(V) = dI(V)/dV$ normalized to their normal-state values G_N as functions of the $eV/(k_BT_c)$ ratio measured at $T = 4.2$ K at the upper surface of the Ta sample before ($P = 0$ kbar) and after ($P \neq 0$ kbar) HPT treatment (*b*). Fitting parameters for calculated $G(V)$ characteristics were $\Delta_0 = 0.39$ meV, $\Gamma_0 = 0$, and $\Delta P = 0.79$ meV, $\Gamma_P = 0.38$ meV, $Z_0 = Z_P = 0$. The ratio of the critical temperatures $T_{cP}/T_{c0} = 1.11$. The indices 0 and P refer to the superconducting states before and after HPT treatment, respectively.

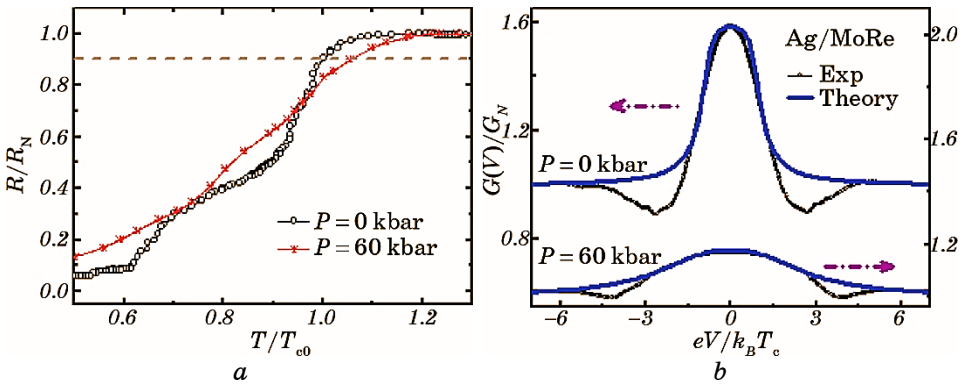

Fig. 3. Ag/MoRe point contact: temperature-dependent resistances normalized to their normal-state values as functions of the T/T_{c0} ratio, where $T_{c0} = T_c(P = 0$ kbar) (*a*) and differential conductance $G(V) = dI(V)/dV$ normalized to their normal-state values G_N as functions of the $eV/(k_BT_c)$ ratio measured at $T = 4.2$ K at the upper surface of the MoRe sample before ($P = 0$ kbar) and after ($P \neq 0$ kbar) HPT treatment (*b*). Fitting parameters for calculated $G(V)$ characteristics were $\Delta_0 = 0.81$ meV, $\Gamma_0 = 0.18$, and $\Delta P = 1.59$ meV, $\Gamma_P = 1.51$ meV, $Z_0 = Z_P = 0$. The ratio of the critical temperatures $T_{cP}/T_{c0} = 1.06$. The indices 0 and P refer to the superconducting states before and after HPT treatment, respectively.

evidence of the profound change in superconducting properties caused by the HPT process, in particular associated with the shear-deformed surface layer, and serves as a basis for a detailed analysis of the role of the amorphization mechanism in enhancing T_c.

The appearance of the differential conductance $G(V)$ as a function of the voltage bias V alone allows us to assess the quality of the contact between N tip and S material being studied. In the case of ideal N/S contact, all electrons injected from the normal metal are reflected as quasi-hole excitations, resulting in the $G(V = 0)$ value doubling compared to the corresponding normal value. If the N/S contact resistance is significant (usually, due to the presence of a metal oxide), the probability of the simultaneous passage of two electrons forming a Cooper's pair through it becomes extremely small, and the conductance at zero bias voltage is negligible. Within the framework of the BTK theory [20], the electron scattering efficiency at the N/S interface is described by a dimensionless parameter Z, which is proportional to the height and width of the potential barrier separating the two metals ($Z = 0$ corresponds to the absence of a barrier). Another governing parameter, which takes into account the smearing of the BCS gap edge singularity and additional states in the sub-gap region due to a finite quasiparticle lifetime, as well as the temperature effect, is known as the Dynes parameter Γ. Thus, the shape of the differential conductance

of an N/S junction normalized to its normal value is described by three parameters: the superconductor energy gap Δ, the effective barrier strength Z, and the Dynes parameter Γ. The captions to Figs. 2 and 3 show their values for studied Ta and MoRe alloy slabs, respectively.

Following our previous article [13], we determined the critical temperature as the onset of the diamagnetic response at a level of $0.9R_N$ where $R_N = 1/G_N$, R_N and G_N are the resistance and conductance in the normal state. In this case, our values of the critical temperature are slightly overestimated compared to most literature data. Here, however, we are interested not so much in the T_c values themselves, but rather in their variations after the HPT treatment and, moreover, in the changes in the ratio of the energy gap Δ, reconstructed from the point-spectroscopy data, to T_c. As is known, this ratio is a characteristic of the electron–phonon coupling strength in the superconductor under study [21]. In both as-prepared films, it equals $2\Delta/T_c = 2.0–2.1$, which is significantly less than the BCS value of 3.528 and can be attributed to the depletion of the superconducting density of states near the surface [22]. However, after HPT processing, the $2\Delta/T_c$ ratio in both superconductors increases to values from 3.7 to 3.8, indicating the presence of moderate electron–phonon coupling. This can be clearly seen from a comparison of the corresponding point-contact measurements (see Fig. 2, *b* and Fig. 3, *b*, where the two normalized $G(V)/G_N(V)$ characteristics are shown as functions of the $eV/(k_BT_c)$ ratios; k_B is the Boltzmann's constant). According to the standard BTK theory [20], the distance between points on a zero-bias peak in the $G(V)$ peak where the intensity is a half of the maximum amplitude provides an estimate of the 2Δ value. Thus, normalization by T_c gives us an estimate of $2\Delta/T_c$. Comparison of the two curves in Fig. 2, *b* and Fig. 3, *b* clearly shows a nearly twofold increase in this ratio, reflecting a noticeable increase in the electron–phonon coupling.

5. AMORPHIZATION IMPACT ON SUPERCONDUCTING CRITICAL PARAMETERS

The influence of amorphization on the critical parameters of superconductors is a complex phenomenon rooted in the principal relationship between a material's structural order and its electronic properties. The process of disrupting a highly-ordered crystal lattice to create a disordered, glass-like state fundamentally alters the environment, in which Cooper's pairs form and travel. This structural disruption can be induced through various methods, including the HPT process. The resulting disorder impacts each of the critical superconducting parameters in distinct, and, sometimes opposing, ways.

The critical temperature T_c is generally highly sensitive to the structural integrity of the material. In a superconductor, T_c is gov-

erned by the electronic density of states at the Fermi level and the phonon spectrum, both of which are intimately tied to the crystal lattice. For many highly optimized crystalline superconductors, such as high-temperature cuprates or specific intermetallic compounds, amorphization destroys the precise crystal symmetry required for their specific pairing mechanisms, leading to a drastic suppression or complete eradication of superconductivity. However, the effect is highly material-dependent. In certain transition metal alloys, the transition to an amorphous state can broaden the electronic density of states. While this smears out sharp peaks that might favour high T_c in a crystal, it can also stabilize the superconducting phase against structural instabilities, resulting in a robust, albeit sometimes lower, critical temperature that is highly resistant.

Generally, the Anderson's theorem provides important theoretical context for understanding these effects since it states that non-magnetic disorder should not suppress T_c in conventional superconductors with *s*-wave pairing, provided the disorder is weak. However, the theorem applies strictly only at zero temperature and in idealized conditions. In real amorphous superconductors, the situation is more nuanced. Strong disorder can break the assumptions underlying Anderson's theorem, while magnetic impurities introduced during amorphization can have severe pair-breaking effects. Additionally, the theorem does not directly address changes in the density of states or the role of disorder in destabilizing the superconducting phase in materials with short coherence lengths or unusual pairing mechanisms. The microscopic mechanisms underlying the amorphization effect involve changes in the electronic density of states at the Fermi level, alterations in electron–phonon coupling strength, and modifications to the superconducting gap structure. In amorphous materials, the absence long-range order results in a broadened density of states and smearing of band edges. This can reduce the effective coupling constant for superconductivity, particularly affecting materials, where the density of states at the Fermi level plays a crucial role in determining T_c. Nevertheless, amorphization can play positive role in superconductors with the dominating impact of the phonon spectrum. In this case, the disorder-caused growth of the electron–phonon interaction strength

$$\lambda = 2\int_0^\infty \alpha^2 F(\omega)\omega^{-1} d\omega,$$

where $\alpha^2 F(\omega)$ is the Eliashberg's electron–phonon spectral function, is controlled by an enhancing role of low-frequency transverse phonon excitations. The significant increase in the $2\Delta/T_c$ ratio under the HTP impact proves that this is just the scenario realized in our experiments. It should be noted that the question of amorphization of two-band superconductors, which include molybdenum–rhenium alloy [23, 24] and

the most famous representative of which is magnesium diboride [25], remains completely open. Definitive answers to the arisen questions are a task for future research.

6. SUMMARY

This study establishes 'bulk twistronics' as a viable and powerful experimental technique. It expands the twistronics concept far beyond the realm of 2*D* van der Waals crystals, proving that rotational degrees of freedom (even when imposed as a macroscopic shear) can serve as a highly effective tuning knob for superconductivity in conventional metallic systems. The continuous and reversible nature of mechanical deformation offers a highly tuneable platform for exploring the stability boundaries of superconducting states and their interplay with lattice degrees of freedom. Furthermore, by comparing two superconductors with fundamentally different electronic characters (a single-band elemental metal versus a two-band alloy), we gain valuable, complementary insights into the mechanisms that govern superconductivity under extreme strain.

Future research in this area should continue exploring the precise mechanisms linking amorphization to critical parameter changes, the role of different types of disorder in various superconducting systems, and the development of materials that significantly enhance superconducting properties despite increased amorphization. We expect that bridging concepts from strain engineering, high-pressure physics, and topological materials science, advanced characterization techniques and theoretical models will refine our understanding of these complex phenomena contributing to both fundamental superconductivity science and practical device development.

This contribution was created under the project No. 0125U000295 (G. V. Kurdyumov Institute for Metal Physics) supported by the National Academy of Sciences of Ukraine. The work by O. Zhitlukhina was supported by the EU NextGenerationEU through the Recovery and Resilience Plan for Slovakia under Projects 09I03-03-V01-00139 and 09I03-03-V01-00140.

AUTHORS' CONTRIBUTIONS

V. Tarenkov developed *in-situ* torsional strain integration for anvil cells and processed superconducting transition temperature and resistivity data. D. Mindich performed transport measurements of Ta and MoRe samples and participated in performing the computational analysis of the obtained data. V. Dmytrenko provided custom miniature torsional strain cell hardware for high-pressure anvil cell integration.

O. Zhitlukhina estimated electron–phonon coupling values in both materials under torsional and hydrostatic load, advised on strain-induced electronic structure modification hypotheses for Ta and MoRe. V. Krivoruchko advised the core team on the unique superconducting properties of two-band/two-gap MoRe alloys, supporting interpretation of non-standard T_c and $2\Delta/T_c$ trends in highly strained samples. O. Kalenyuk developed high-purity Ta and MoRe sample synthesis protocols and characterization of the samples. D. Shapovalov participated in the computational analysis of the obtained data of transport measurements. V. Shamaev carried out mathematical processing of the obtained experimental data and modelling of the superconductors' amorphization. A. Shapovalov supervised the project, devised the main conceptual ideas, controlled experimental results, and provided critical feedback. All authors approved the final version of the manuscript.

REFERENCES

1. S. S. Dindorkar, A. S. Kurade, and A. H. Shaikh, *Chem. Phys. Impact*, **7**: 100325 (2023).
2. F. Escudero, D. Wang, P. A. Pantaleyn, S. Yuan, F. Guinea, and Z. Zhan, *arXiv:2602.02692 [cond-mat.mes-hall]* (2026).
3. J. Attig, J. Park, M. M Scherer, S. Trebst, A. Altland, and A. Rosch, *2D Mater.*, **8**: 044007 (2021).
4. D. Zhai, H. Yu, and W. Yao, *Rep. Prog. Phys.*, **88**: 084501 (2025).
5. J. Yang, S. Wang, K. Wang, Y. Fang, H. Wang, L. Wang, H. Xing, and P. Hu, *Int. J. Refract. Met. Hard Mater.*, **134**: 107408 (2026).
6. K. Edalati and Z. Horita, *Mater. Sci. Eng. A*, **652**: 325 (2016).
7. K. Edalati, A. Bachmaier, V. A. Beloshenko, Y. Beygelzimer, V. D. Blank, W. J. Botta, K. Bryła, J. Čížek, S. Divinski, N. A. Enikeev, Yu. Estrin, G. Faraji, R. B. Figueiredo, M. Fuji, T. Furuta, T. Grosdidier, J. Gubicza, A. Hohenwarter, Z. Horita, J. Huot, Y. Ikoma, M. Janeček, M. Kawasaki, P. Král, S. Kuramoto, T. G. Langdon, D. R. Leiva, V. I. Levitas, A. Mazilkin, M. Mito, H. Miyamoto, T. Nishizaki, R. Pippan, V. V. Popov, E. N. Popova, G. Purcek, O. Renk, Á. Révész, X. Sauvage, V. Sklenicka, W. Skrotzki, B. B. Straumal, S. Suwas, L. S. Toth, N. Tsuji, R. Z. Valiev, G. Wilde, M. J. Zehetbauer, and X. Zhu, *Mater. Res. Lett.*, **10**: 163 (2022).
8. Y. Beygelzimer, Y. Estrin, and R. Kulagin, *Mater. Trans.*, **64**: 1856 (2023).
9. M. Mito, H. Matsui, K. Tsuruta, T. Yamaguchi, K. Nakamura, H. Deguchi, N. Shirakawa, H. Adachi, T. Yamasaki, H. Iwaoka, Y. Ikoma, and Z. Horita, *Sci. Rep.*, **6**: 36337 (2016).
10. T. Nishizaki, K. Edalati, S. Lee, Z. Horita, T. Akune, T. Nojima, S. Iguchi, and T. Sasaki, *Mater. Trans.*, **60**: 1367 (2019).
11. M. Mito, S. Shigeoka, H. Kondo, N. Noumi, Y. Kitamura, K. Irie, K. Nakamura, S. Takagi, H. Deguchi, T. Tajiri, M. Ishizuka, T. Nishizaki, K. Edalati, and Z. Horita, *Mater. Trans.*, **60**: 1472 (2019).
12. M. Mito, N. Mokutani, Y. Tang, K. Matsumoto, T. Tajiri, and Z. Horita, *J. Mater. Sci.*, **59**: 5981 (2024).

13. V. Tarenkov, V. Krivoruchko, A. Shapovalov, O. Kalenyuk, I. Martynenko, V. Dmytrenko, E. Zhitlukhina, and M. Belogolovskii, *Low Temp. Phys.*, **51**: 850 (2025).
14. J. Kang, H. Yang, Q. Hu, Z. Cai, L.-M. Liu, and L. Guo, *Chem. Rev.*, **123**: 8859 (2023).
15. G. Liu and H. Huang, *Front. Mater.*, **12**: 1589830 (2025).
16. C. Lin, B. Wang, and K. H. Teo, *Physica C*, **532**: 27 (2017).
17. M. Baggioli, C. Setty, and A. Zaccone, *Phys. Rev. B*, **101**: 214502 (2020).
18. X. Y. Li, H. P. Zhang, S. Lan, D. L. Abernathy, C. H. Hu, L. R. Fan, M. Z. Li, and X.-L. Wang, *Nature Commun.*, **17**: 860 (2026).
19. Yu. G. Naidyuk and I. K. Yanson, *Point-Contact Spectroscopy* (New York: Springer: 2005).
20. G. E. Blonder, M. Tinkham, and T. M. Klapwijk, *Phys. Rev. B*, **25**: 4515 (1982).
21. V. Z. Kresin, *Solid State Commun.*, **63**: 725 (1987).
22. E. Khestanova, J. Birkbeck, M. Zhu, Y. Cao, G. L. Yu, D. Ghazaryan, J. Yin, H. Berger, L. Forry, T. Taniguchi, K. Watanabe, R. V. Gorbachev, A. Mishchenko, A. K. Geim, and I. V. Grigorieva, *Nano Lett.*, **18**: 2623 (2018).
23. V. Tarenkov, A. Dyachenko, V. Krivoruchko, A. Shapovalov, and M. Belogolovskii, *J. Supercond. Nov. Magn.*, **33**: 569 (2020).
24. V. Tarenkov, A. Shapovalov, E. Zhitlukhina, M. Belogolovskii, and P. Seidel, *Low Temp. Phys.*, **49**: 103 (2023).
25. T. A. Prikhna, A. P. Shapovalov, G. E. Grechnev, V. G. Boutko, A. A. Gusev, A. V. Kozyrev, M. A. Belogolovskii, V. E. Moshchil, and V. B. Sverdun, *Low Temp. Phys.*, **42**: 380 (2016).